Available online at http://scik.org
J. Math. Comput. Sci. 11 (2021), No. 4, 4563-4585
https://doi.org/10.28919/jmcs/5719
ISSN: 1927-5307

NUMERICAL SOLUTION OF THE VOLTERRA-FREDHOLM INTEGRAL EQUATION BY THE FRAMELET METHOD

ABDALLAH AL-HABAHBEH*

Department of Mathematics, Tafila Technical University, Tafila, Jordan

Abstract. In this paper, a numerical method is proposed to solve the Volterra-Fredholm Integral Equation. The method is based on the use of framelets to reduce the integral equation to a system of algebraic equations, a numerical solution is given by using collocation method.

Finally, numerical examples are presented to test the efficiency of the proposed method. Comparative results show that our method is more accurate than existing ones.

Keywords: tight framelets; multiresolution analysis; unitary extension principle; oblique extension principle; B-spline; collocation method.

2010 AMS Subject Classification: 65R10, 65R20, 65T60.

1. Introduction

Framelets have been widely researched in literature and have been successfully extended to many applications, for example, the redundant representation offered by the tight framelet, made it a beneficial tool in signal processing [1] and image compression and restoration [2]. Several articles have shown that constructing and building tight framelets, is much simpler and more versatile than orthonormal wavelet bases [3], [4], [5].

*Corresponding author

E-mail address: aaalhaba@ttu.edu.jo

Received March 18, 2021

In this paper, tight framelets extracted from refinable functions via a Multiresolution Analysis (MRA) are of special interest to us. The concept of Hilbert space frame was first introduced in 1952 by Duffin and Schaffer [6], where nonharmonic Fourier series has been discussed. The topic has been revived in 1986 by Daubechies, Grossmann,and Meyer in [7] where they gave a solid mathematical basis to the discrete wavelets. Ron and Shen in [8] offered a general characterization of all framelets, concentrating on tight framelets. The authors in [9] discussed frames from a numerical analysis point of view and concluded that truncated frames often result ill-conditioned linear system.

Several articles emphasis on framelets built through MRA and extension principles, as this ensures the presence of fast frames algorithms for application, refer to [10] [11]. MRA symmetric tight framelets resulting from symmetric refinable functions are of interest in both theory and applications.

Many problems that appear to handled with ordinary and partial differential equations can be recast as integral equations, as well as, being useful tool to state many problems in mathematical physics. One of these is Volterra-Fredholm Integral Equation (VFIE) which usually occur from the mathematical modelling of the spatiotemporal growing of some epidemics and from the theory of nonlinear boundary value problems.

The method of separation of variables has been used in [12] to convert (VFIE) of the second kind to the Volterra Integral Equation of the second kind. The author in [13] used the framelets to give a numerical solution of the Volterra Integral Equation. Amin et al. [14] developed a numerical technique to solve the delay (VFIE) by using Haar wavelet. Method based on the two dimensional Legendre wavelets has been presented in [15] to approximate the solution of the Mixed Voltera-Fredholm Integral Equation (MVFIE) . Wazwaz [16] presented a method for solving (MVFIE) using Adomian decomposition series. In [17], biorthogonal tight framelets are used to solve weakly singular (MVFIE).

The standard form of the Volterra-Fredholm integral is given by

$$u(x) = f(x) + \int_a^x K_1(x,t)u(t)dt + \int_a^b K_2(x,t)u(t)dt,$$

where u is an unknown function and $K_1(x,t)$ and $K_2(x,t)$ are the kernels of the equation.

The paper is organized as follows. In Section 2 we present some concepts and properties of framelets. Then we turn to MRA and the related extension principles, as well as, tight framelets based on B-spline in Section 3. The proposed method is introduced in Section 4. We conclude this paper (Section 5) with some numerical examples to provide the efficiency of the method.

2. Definitions and Basics

The main purpose of this section is to introduce some basic notations and concepts.
The support of the function f is defined by

$$supp\, f := \overline{\{x \in \mathbb{R} : f(x) \neq 0\}}.$$

For $1 \leq p < \infty$, $L^p(\mathbb{R})$ is defined by

$$L^p(\mathbb{R}) := \{f : \mathbb{R} \to \mathbb{C} : f \text{ is measurable and } \int_{\mathbb{R}} |f(x)|^p dx < \infty\}.$$

The definition of frame is what follows:

Definition 2.1. A sequence $\{f_k\}_{k=1}^{\infty}$ of elements in $L^2(\mathbb{R})$ is a frame for $L^2(\mathbb{R})$ if there exist constants, A, $B > 0$ such that

$$A\|f\|^2 \leq \sum_{k=1}^{\infty} |\langle f, f_k\rangle|^2 \leq B\|f\|^2, \qquad \forall f \in L^2(\mathbb{R}),$$

where $|\langle f,g\rangle| := \int_{\mathbb{R}} f(x)\overline{g(x)}dx$ and $\|f\|^2 := |\langle f,f\rangle|$. The numbers A, B are called the lower and upper frame bounds, respectively. A frame which is not a basis is said to be redundant. A frame is called a tight frame if $A = B$; in case $A = 1$, it is called a Parseval frame. In fact, if $\{f_k\}_{k=1}^{\infty}$ is a tight frame for $L^2(\mathbb{R})$, then

$$\sum_{k=1}^{\infty} |\langle f, f_k\rangle|^2 = A\|f\|^2, \qquad \forall f \in L^2(\mathbb{R}),$$

and

$$f = \frac{1}{A}\sum_{k=1}^{\infty} |\langle f, f_k\rangle| f_k\,, \qquad \forall f \in L^2(\mathbb{R}).$$

Note that one can extend the functions in a frame for $L^2(a,b)$ to functions in $L^2(\mathbb{R})$, by defining them to be zero on $\mathbb{R}\backslash(a,b)$ gives a frame for $L^2(\mathbb{R})$. On the other hand, restricting the functions in a frame for $L^2(\mathbb{R})$ to the interval (a,b) gives a frame for $L^2(a,b)$.

For $f \in L^1(\mathbb{R})$, the Fourier transform of f is defined by

$$\mathscr{F} f = \hat{f}(\gamma) := \int_{\mathbb{R}} f(x) e^{-ix\gamma} dx, \qquad \gamma \in \mathbb{R}.$$

Given two functions $f, g \in L^1(\mathbb{R})$, the convolution $f * g$ is defined by

$$f * g(y) := \int_{\mathbb{R}} f(y-x) g(x) dx, \qquad y \in \mathbb{R},$$

with the property that $\widehat{f*g}(\gamma) = \hat{f}(\gamma)\hat{g}(\gamma) \quad \forall \gamma \in \mathbb{R}$.

Let $l_2(\mathbb{Z})$ be the set of all sequences $h = \{h_k\}$ defined on $\mathbb{Z}$ such that

$$l_2(\mathbb{Z}) = \{\{h_k\}_{k\in\mathbb{Z}} : h_k \in \mathbb{C}, \sum_{k\in\mathbb{Z}} |h_k|^2 < \infty\}.$$

The Fourier series for $h \in l_2(\mathbb{Z})$ is given by

$$\hat{h}(\gamma) = \sum_{k\in\mathbb{Z}} h_k e^{-ik\gamma}, \quad a.e.\ \gamma \in \mathbb{R}.$$

The bracket product of two functions $f, g \in L^2(\mathbb{R})$, denoted by $[f,g]$, and defined by

$$[f,g](x) = \sum_{k\in 2\pi\mathbb{Z}} f(x+k)\overline{g(x+k)}.$$

For any closed subset S in $L^2(\mathbb{R})$ and any function $f \in L^2(\mathbb{R})$, the approximation error is

$$E(f,S) := min\{||f-s|| : s \in S\}.$$

A function ϕ is said to be refinable if it satisfies the refinement equation

$$\phi(x) = 2\sum_{k\in\mathbb{Z}} h_0[k]\ \phi(2x-k), \tag{1}$$

for some $h_0 \in l_2(\mathbb{Z})$, called the refinement mask of ϕ. In Frequency (Fourier) domain, the definition of refinability of ϕ can be written as

$$\hat{\phi}(\gamma) = \hat{h}_0(\gamma/2)\ \hat{\phi}(\gamma/2). \tag{2}$$

Throughout this paper, we assume that $\hat{h}_0(0) = 1$ and all sequences on $\mathbb{Z}$ are assumed to be real-valued. Consequently, it follows from (2) that $\hat{\phi}(\gamma) = \prod_{k=1}^{\infty} h_0(2^{-k}\gamma)$.

Next, the definition of some important operators in $L^2(\mathbb{R})$ is given:

Definition 2.2. Given a function $f \in L^2(\mathbb{R})$, we define the following operators:

Translation by a: $T_a f(x) = f(x-a)$, for $a \in \mathbb{R}$;

Dilation or scaling by a: $D_a f(x) = \frac{1}{\sqrt{a}} f(\frac{x}{a})$, for $a \in \mathbb{R}\backslash\{0\}$;

and the dyadic scaling operator is given by

$$(Df)(x) = D_{1/2}f(x) = 2^{1/2} f(2x), x \in \mathbb{R}.$$

The following is important relation between the operators:

$$T_b D_a f(x) = D_a T_{b/a} f(x) = \frac{1}{\sqrt{|a|}} f(\frac{x}{a} - \frac{b}{a}),$$

which implies that for $j,k \in \mathbb{Z}$

$$T_k D^j = D^j T_{2^j k} \text{ and } D^j T_k = T_{2^{-j}k} D^j.$$

For $j,k \in \mathbb{Z}$, define

$$\psi_{j,k}(x) = D^j T_k \psi = 2^{j/2} \psi(2^j x - k), \qquad \forall \psi \in L^2(\mathbb{R}).$$

If $\{\psi_{j,k}\}_{j,k\in\mathbb{Z}}$ is an orthonormal basis for $L^2(\mathbb{R})$, then the function ψ is called a wavelet.

For a set $\{\psi_1, \ldots, \psi_r\}$ of compactly supported functions in $L^2(\mathbb{R})$, we say that $\{\psi_1, \ldots, \psi_r\}$ has m vanishing moments if

$$\int_{\mathbb{R}} x^k \psi_l(x)\, dx = 0 \qquad l = 1, \ldots, r \text{ and } k = 0, \ldots, m-1.$$

Definition 2.3. Given $\Psi = \{\psi_1, \ldots, \psi_r\} \subset L^2(\mathbb{R})$, define the dyadic wavelet system or affine system $X(\Psi)$ as

$$X(\Psi) = \{\psi_{l,j,k} : 1 \leq l \leq r,\ j,k \in \mathbb{Z}\},$$

where $\psi_{l,j,k} = D^j T_k \psi_l$. This system is called a wavelet frame (framelet) of $L^2(\mathbb{R})$ if there exist constants, A, $B > 0$ such that

$$A\|f\|^2 \leq \sum_{g \in X(\Psi)} |\langle f, f_k \rangle|^2 \leq B\|f\|^2, \qquad \forall f \in L^2(\mathbb{R}).$$

In the case where $X(\Psi)$ is a tight framelet with bound one, we have the perfect reconstruction property

$$f = \sum_{g\in X(\Psi))} |\langle f, g\rangle| g. \quad \forall f \in L^2(\mathbb{R}),$$

which can be written in particular as

$$f = \sum_{l=1}^{r} \sum_{j\in\mathbb{Z}} \sum_{k\in\mathbb{Z}} |\langle f, \psi_{l,j,k}\rangle| \psi_{l,j,k}. \quad \forall f \in L^2(\mathbb{R}).$$

The elements of Ψ, i.e., $\psi_1, \ldots, \psi_r$ are called the generators for the corresponding framelet. A significant property of a framelet system is the order of vanishing moments. The framelet system has vanishing moments of order m_0 if, for each $\psi_l \in \Psi$, $\hat{\psi}_l$ has a zero of order m_0 at the origin.
Let $X(\Psi)$ be a tight frame system, we define the truncated operator $\mathscr{Q}_n$ by

$$\mathscr{Q}_n : f \mapsto \sum_{\psi\in\Psi,\, k\in\mathbb{Z},\ j<n} |\langle f, \psi_{l,j,k}\rangle| \psi_{l,j,k}.$$

We say that the tight frame system $X(\Psi)$ provides approximation order m_1, if, for all f in the Sobolve space $\mathscr{W}_2^m(\mathbb{R})$,

$$\|f - \mathscr{Q}_n\|_{L^2(\mathbb{R})} = \mathscr{O}(2^{-nm_1})$$

A subspace $S \subset L^2(\mathbb{R})$ is called a shift-invariant if for any $k \in \mathbb{Z}$ and $f \in S$, we have $f(.-k) \in S$. Shift-invariant spaces are important in construction of applicable framelets. Notice that the affine framelet system $X(\Psi)$ is not shift-invariant. To associate this system with another shift-invariant system, Ron and Shen in [8] introduced a notation of quasi-affine system.

Definition 2.4. Given $\Psi = \{\psi_1, \ldots, \psi_r\}$. A quasi-affine system from level L is defined by

$$X_L^q(\Psi) := \{\psi_{l,j,k}^q : 1 \le l \le r,\ j,k \in \mathbb{Z}\},$$

where $\psi_{l,j,k}^q$ is given by

$$\psi_{l,j,k}^q = \begin{cases} D^j T_k \psi_l, & j \ge L \\ 2^{\frac{j-L}{2}} T_{2^{-L}k} D^j \psi_l, & j < L \end{cases}.$$

The system $X_L^q(\Psi)$ is a 2^{-L} shift-invariant system. The approximation order is the same for the affine system and it's corresponding quasi-affine system.

In our discussion below, we need to define the spectrum of the shift-invariant space V_0 as

$$\sigma(V_0) := \{\gamma \in [-\pi, \pi] : \hat{\phi}(\gamma + 2\pi k) \neq 0, \text{ for some } k \in \mathbb{Z}\},$$

and it is determined only up to a null set. In fact, if ϕ is compactly supported, then $\sigma(V_0) = [-\pi, \pi]$.

3. Tight Framelets via MRA

In this section, we discuss tight framelets designed via MRA. Principally, we provide general basis and specific algorithms for tight framelets, and we discuss how they can used for building B-spline tight framelets. Several explicit examples are presented.

3.1. Multiresolution Analysis. Multiresolution Analysis (MRA) were developed by Mallat and Meyer in 1986 as a general method to generate wavelet orthonormal bases for $L^2(\mathbb{R})$ of the form $\{2^{j/2}\psi(2^j x - k)\}_{j,k\in\mathbb{Z}}$. Tight framelets that have a (MRA) setup are preferred in applications because this guarantees the existence of fast decomposition and reconstruction algorithms [11].

In this paper, we adopt a MRA setup as proposed in [10], rather than the original setup.

Given $\phi \in L^2(\mathbb{R})$ and define the shift-invariant subspace $V_0(\phi) \subset L^2(\mathbb{R})$ by

$$V_0 := V_0(\phi) = \overline{span}\{T_k\phi\}_{k\in\mathbb{Z}},$$

and set

$$V_j := D^j V_0(\phi).$$

The function ϕ is said to generate the MRA $(V_j)_{j\in\mathbb{Z}}$ if

$$V_0 \subset V_1;$$

$$\overline{\cup_{j\in\mathbb{Z}} V_j} = L^2(\mathbb{R});$$

$$\cap_{j\in\mathbb{Z}} V_j = \{0\},$$

hold.

A wavelet system $X(\Psi)$ is said to be MRA based for $L^2(\mathbb{R})$ if there exists an MRA sequence of subspaces $\{V_j\}_{j\in\mathbb{Z}}$ such that the condition $\Psi \subset V_1$ holds. If, in addition, the system $X(\Psi)$ is a frame, we refer to its elements as framelets.

The generator ϕ of the MRA is known as a refinable function or a scaling function. It has been demonstrated in literature that the approximation properties of a shift-invariant space are related to the order of the zeros of $\hat{\phi}$ at $2\pi k, k \in \mathbb{Z}$. Therefore it is important to examine the behavior near zero of the 2π-periodization of $|\hat{\phi}|^2$, i.e., $[\hat{\phi},\hat{\phi}] = \sum_{k\in 2\pi\mathbb{Z}} |\hat{\phi}(.+k)|^2$.

In this paper, we assume that ϕ is a compactly supported refinable function generated by a finitely supported refinement mask and satisfy the following:

(i) $\phi(0) = 1$.

(ii) $\lim_{\omega\to 0}\hat{\phi}(\omega) = 1$.

(iii) $[\hat{\phi},\hat{\phi}]$ is essentially bounded.

Based on (2), the refinement mask $\hat{h}_0$ completely determine ϕ and therefore the underlying MRA.

Further, define $\psi_l \in L^2(\mathbb{R})$ by

$$\psi_l(x) = 2\sum_{k\in\mathbb{Z}} h_l[k]\phi(2x-k), \qquad l = 1,\ldots,r, \tag{3}$$

which can be written in frequency domain as

$$\hat{\psi}_l(\gamma) = \hat{h}_l(\gamma/2)\hat{\phi}(\gamma/2), \qquad l = 1,\ldots,r.$$

The periodic measurable functions $\hat{h}_1,\ldots,\hat{h}_r$ are called wavelet masks or masks.

The MRA provides approximation order m, if, for every $f \in \mathscr{W}_2^m(\mathbb{R})$,

$$dist(f,V_j) := min\{\|f-g\|_{L^2(\mathbb{R})} : g \in V_j\} = \mathscr{O}(2^{-jm}.) \tag{4}$$

In the following we present some important extensions of the original MRA. The main purpose of these extensions is to construct tight framelets with prescribed properties.

3.2. Extension Principles. The main extensions to MRA are given in this subsection: The Unitary Extension Principle (UEP) and the Oblque Extension Principle (OEP). The aim is to construct functions $\psi_1,\ldots,\psi_n$ belonging to V_1 such that $\{\psi_{l;j,k}\}_{j,k\in\mathbb{Z},l=1,2,\ldots,r}$ forms a tight frame for $L^2(\mathbb{R})$.

First, let us define the fundamental function Θ by

$$\Theta(\gamma) := \sum_{j=0}^{\infty}\sum_{i=1}^{r} |\hat{h}_i(2^j\gamma)|^2 \prod_{m=0}^{j-1} |\hat{h}_0(2^m\gamma)|^2. \tag{5}$$

The definition of Θ ensures

$$\Theta(\gamma) = \sum_{j=1}^{r} |\hat{h}_j(\gamma)|^2 + |\hat{h}_0(\gamma)|^2\Theta(2\gamma).$$

The following UEP has been introduced and proved by Daubechies et al. [10].

Theorem 3.1. *Let ϕ be a compactly supported refinable function in $L^2(\mathbb{R})$ with refinement mask $\hat{h}_0 \in l_2(\mathbb{Z})$. Suppose that there exist a sequence of measurable and essentially bounded functions $\{\hat{h}_l\}_{l=1}^{r}$. Assume that, for almost all $\gamma \in \sigma(V_0)$, and all $\nu \in [0,\pi]$,*

$$\sum_{l=0}^{r} \hat{h}_l(\gamma)\overline{\hat{h}_l(\gamma+\nu)} = \begin{cases} 1, & \nu = 0 \\ 0, & otherwise \end{cases}$$

Then the resulting wavelet system $X(\Psi)$ is a tight frame in $L^2(\mathbb{R})$, and the fundamental function Θ equals 1 a.e. on $[-\pi,\pi]$.

The UEP is shown to be a very beneficial method to construct compactly supported spline framelets, but the generators have some constraints, e.g. on the number of vanishing moments. For more details, refer to [18]. In fact, when the number of vanishing moments increases, the framelet representation of one-dimensional piecewise-smooth functions become sparser.

The primary purpose of the following theorem of Oblique Extension Principle (OEP) is to increase vanishing moments of masks derived from a given refinement mask. This principle was first presented and proved in [10]

Theorem 3.2. *Let ϕ be a compactly supported refinable function in $L^2(\mathbb{R})$ with refinement mask $\hat{h}_0 \in l_2(\mathbb{Z})$. Assume there exists a 2π-periodic function Θ that satisfies the following:*

(1) Θ is non-negative, essentially bounded, continuous at the origin, and $\Theta(0) = 1$.

(2) If $\gamma \in [-\pi,\pi]$ and $\nu \in [0,\pi]$ is such that $\gamma+\nu \in [-\pi,\pi]$, then

$$\hat{h}_0(\gamma)\overline{\hat{h}_0(\gamma+\nu)}\Theta(2\gamma)+\sum_{l=1}^{r}\hat{h}_l(\gamma)\overline{\hat{h}_l(\gamma+\nu)} = \begin{cases}\Theta(\gamma), & \nu = 0\\ 0, & otherwise.\end{cases}$$

Then the system $X(\Psi)$ defined by $\hat{h}_0,\ldots,\hat{h}_r$ is a tight framelet in $L^2(\mathbb{R})$.

The oblique extension principle can be used to obtain spline tight frame system whose truncated framelet system has high approximation order and whose generators have high order vanishing moments.

Lemma 3.3. *Let $X(\Psi)$ be an MRA tight frame system with generator ϕ provides approximation order m. Then the approximation order of the framelet system is* $\min\{m,m'\}$*, with m' is the order of the zero of $\Theta(.)-\Theta(2.)|\hat{h}_0|^2$ at the origin.*

Proof. refer to [10]. □

Lemma 3.4. *The MRA-based wavelet system $X(\Psi)$ has vanishing moments of order m_0 if and only if $\sum_{j=1}^{r}|\hat{h}_j(\gamma)|^2 = \mathscr{O}(|\gamma|)^{2m_0}$, near the origin.*

Proof. Since $\hat{\psi}_l(\gamma) = \hat{h}_l(\gamma)\hat{\phi}(\gamma/2)$ and $\hat{\phi}(0) = 1$, i.e., $\hat{\psi}_l(0) = \hat{h}_l(0)$, the vanishing moments of ψ_l are determined completely by the order of the zero (at the origin) of $\hat{h}_l$. Hence, $X(\Psi)$ has vanishing moments of order m_0 is equivalent to

$$\sum_{l=1}^{r}|\hat{h}_l(\gamma)|^2 = \mathscr{O}(|\gamma|^{2m_0})$$

□

Next, we show that the approximation order of the MRA provides an upper bound for the approximation order of it's corresponding framelet system.

Theorem 3.5. *Let $X(\Psi)$ be an MRA tight frame system. Assume that the system has vanishing moments of order m_0, and that the refinable function ϕ provides approximation order m. Then the approximation order of the tight frame system is min$\{m,2m_0\}$.*

Proof. Let $X(\Psi)$ be a tight framelet. Hence, it is satisfy the OEP conditions, and thus

$$\sum_{j=1}^{r} |\hat{h}_j(\gamma)|^2 = \Theta(\gamma) - |\hat{h}_0(\gamma)|^2 \Theta(2\gamma).$$

It follows that m' in Lemma 3.3 is $2m_0$. □

3.3. Tight Framelets From B-spline functions. In this subsection, we first review the definition of B-splines functions. Next, we construct tight framelets with several number of generators derived from B-spline functions. B-spline functions, as an essential family of refinable functions, are convenient in applications.

The B-spline of order m, denoted by B_m and defined in frequency domain by

$$|\hat{B}_m(\gamma)| = \left| \frac{\sin(\gamma/2)}{\gamma/2} \right|^m,$$

and its refinement mask is defined by

$$\hat{h}_0(\gamma) = \left(\frac{1+e^{-i\gamma}}{2} \right)^m.$$

In the time domain, the B_m may defined recursively via

$$B_1(x) = \chi_{[0,1]}(x),$$

$$B_{m+1}(x) = B_m * B_1(x), \quad m \in \mathbb{N},$$

with support on $[0,m]$.

Explicit expressions for the piecewise linear $B_2(x)$ and cubic $B_4(x)$ are given by

$$B_2(x) = \begin{cases} x, & x \in [0,1), \\ 2-x, & x \in [1,2), \\ 0, & \text{otherwise} \end{cases}$$

and

$$B_4(x) = \begin{cases} \frac{1}{6}x^3, & x \in [0,1), \\ -\frac{1}{2}x^3 + 2x^2 - 2x + \frac{2}{3}, & x \in [1,2), \\ \frac{1}{2}x^3 - 4x^2 + 10x - \frac{22}{3}, & x \in [2,3), \\ -\frac{1}{6}x^3 + 2x^2 - 8x + \frac{32}{3}, & x \in [3,4), \\ 0, & \text{otherwise.} \end{cases}$$

Now, one can define the m (2π periodic) masks by

$$\hat{h}_l(\gamma) = i^l e^{-im\gamma/2} \sqrt{\binom{m}{l}} \sin^l(\gamma/2) \cos^{m-l}(\gamma/2); \qquad l = 1, \ldots, m. \tag{6}$$

As a result, the m framelets are given by

$$\hat{\psi}_l(\gamma) = i^l e^{-im\gamma/2} \sqrt{\binom{m}{l}} \frac{\cos^{m-l}(\gamma/4) + \sin^{m+l}(\gamma/4)}{(\gamma/4)^m}; \qquad l = 1, \ldots, m \tag{7}$$

The complex number of absolute value 1, i.e., i^l is to guarantee that each of the framelets is a real- valued symmetric (or anti-symmetric) function. Note that the framelets are supported in $[-m,m]$ and they are splines of order $m-1$.

It is known [10], that in order to construct tight framelets that provide high approximation order, we should choose the fundamental function Θ in OEP as a suitable approximation, at the origin, to $1/|\hat{\phi}|^2$. Hence, if $\phi = B_m$, then we should choose Θ as a 2π-periodic function which approximate

$$\left| \frac{\gamma/2}{\sin(\gamma/2)} \right|^{2m}$$

at the origin (see [10] for more results and analysis).

We now give two examples of framelets: Linear, respectively, cubic spline framelets constructed via Theorem 3.1.

Example 3.1. [Tight framelet with two generators by using UEP] Consider the compactly supported refinable function $\phi = B_2(x)$ with the refinement mask $\hat{h}_0(\gamma) = \frac{(1+e^{-i\gamma})^2}{4}$. Define the masks $\hat{h}_1$ and $\hat{h}_2$ by

$$\hat{h}_1(\gamma) = \frac{\sqrt{2}}{4}(1 - e^{-2i\gamma}),$$
$$\hat{h}_2(\gamma) = \frac{-1}{4}(1 - e^{-i\gamma})^2.$$

Consequently

$$\psi_1 = \frac{1}{\sqrt{2}}(B_2(2x) - B_2(2x-2)),$$

$$\psi_2 = \frac{-1}{2}(B_2(2x) - 2B_2(2x-1) + B_2(2x-2)).$$

One can verify that all the conditions in UEP hold and, therefor, the system $X(\{\psi_1, \psi_2\})$ is a tight frame for $L^2(\mathbb{R})$ with two compactly supported symmetric (anti-symmetric) generators (see Figure 1). Although ψ_2 has two vanishing moment, the framelet system has $m_0 = 1$ vanishing moment. The approximation order of the MRA (refinable function $\phi = B_2$) is $m = 2$. The approximation order of the framelet system $X(\{\psi_1, \psi_2\})$ equals $min(m, 2m_0) = 2$.

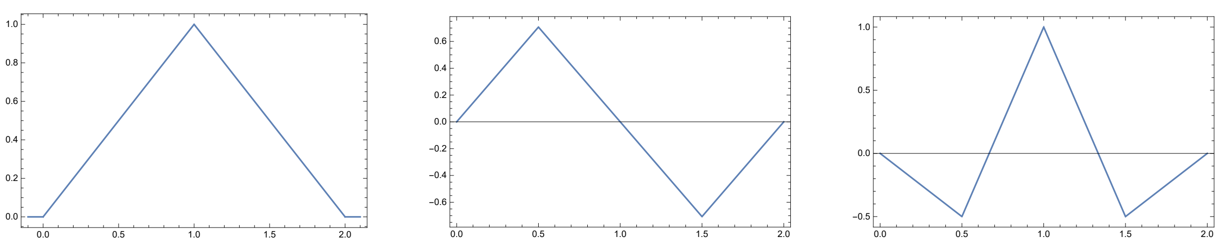

(A) $B_2(x)$ (B) ψ_1 (C) ψ_2

FIGURE 1. The graphs of the piecewise linear B-spline, $B_2(x)$, and corresponding framelets ψ_1 and ψ_2.

Example 3.2. [Tight framelet with four generators by using UEP] Consider $\phi = B_4(x)$ with the refinement mask $\hat{h}_0(\gamma) = \frac{(1+e^{-i\gamma})^4}{16}$. Define the masks as follows

$$\hat{h}_1(\gamma) = -\frac{1}{4}(1-e^{-i\gamma})(1+e^{-i\gamma})^3, \quad \hat{h}_2(\gamma) = -\frac{\sqrt{6}}{16}(1-e^{-i\gamma})^2(1+e^{-i\gamma})^2,$$

$$\hat{h}_3(\gamma) = -\frac{1}{4}(1-e^{-i\gamma})^3(1+e^{-i\gamma}), \hat{h}_4(\gamma) = \frac{1}{4}(1-e^{-i\gamma})^4.$$

Consequently

$$\psi_1(x) = -\frac{1}{2}(B_4(2x) + 2B_4(2x-1) - 2B_4(2x-3) - B_4(2x-4));$$

$$\psi_2(x) = -\frac{\sqrt{6}}{8}(B_4(2x) - 2B_4(2x-2) + B_4(2x-4));$$

$$\psi_3(x) = -\frac{1}{2}(B_4(2x) - 2B_4(2x-1) + 2B_4(2x-3) - B_4(2x-4));$$

and

$$\psi_4(x) = \frac{1}{2}(B_4(2x) - 4B_4(2x-1) + 6B_4(2x-2) - 4B_4(2x-3) + B_4(2x-4)).$$

The system $X(\{\psi_1, \psi_2\, \psi_3, \psi_4\})$ (see Figure 2) is a tight frame for $L^2(\mathbb{R})$ that has vanishing moments of order $m_0 = 1$ since ψ_1 has one vanishing moment. For the refinable function $\phi = B_4$ we have $m = 4$. The approximation order of the framelet system is $min\{4,2\} = 2$.

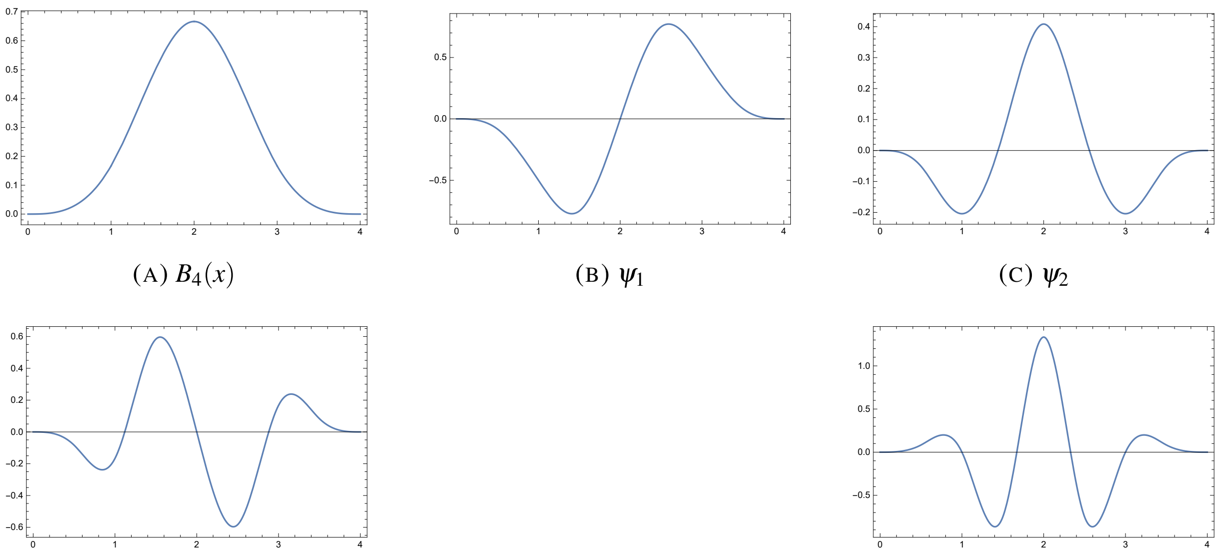

(A) $B_4(x)$ (B) ψ_1 (C) ψ_2

(D) ψ_3 (E) ψ_4

FIGURE 2. The graphs of the piecewise cubic B-spline, $B_4(x)$, and the corresponding framelets

The next example is piecewise cubic spline framelet constructed by using Theorem 3.2.

Example 3.3. [Tight framelet with three generators by using OEP] We return to $\phi = B_4$ in the previous example but now we define the fundamental function Θ to be

$$\Theta(\gamma) = \frac{2452}{945} - \frac{1657}{840}cos(\gamma) + \frac{44}{105}cos(2\gamma) - \frac{311}{7560}cos(3\gamma),$$

and let

$$\hat{h}_1(\gamma) = \tau_1(1-e^{-i\gamma})^4[1+8e^{-i\gamma}+e^{-2i\gamma}],$$

$$\hat{h}_2(\gamma) = \tau_2(1-e^{-i\gamma})^4[1+8e^{-i\gamma}+\tau^* e^{-2i\gamma}+8e^{-3i\gamma}+e^{-4i\gamma}],$$

$$\hat{h}_3(\gamma) = \tau_3(1-e^{-i\gamma})^4[1+8e^{-i\gamma}+(21+\tau/8)(e^{-2i\gamma}+e^{-4i\gamma})+\tau e^{-3i\gamma}+8e^{-5i\gamma}+e^{-6i\gamma}],$$

where

$$\tau^* = \frac{7775}{4396}\tau - \frac{53854}{1099},\ \tau = 317784/7775 + 56\sqrt{168771}/7775 \text{ and}$$

$$\tau_1 = \frac{\sqrt{11113747578360 - 245493856965\tau}}{62697600},$$

$$\tau_2 = \frac{\sqrt{1543080 - 32655\tau}}{40320},$$

$$\tau_3 = \sqrt{32655}/20160.$$

Hence, the symmetric framelets are given by (see Figure 3)

$$\psi_1(x) = 2\tau_1(B_4(2x) + 4B_4(2x-1) - 25B_4(2x-2) + 40B_4(2x-3) - 25B_4(2x-4) + 4B_4(2x-5) + B_4(2x-6)),$$

$$\psi_2(x) = 2\tau_2(B_4(2x) + 4B_4(2x-1) + (\tau^* - 26)B_4(2x-2) + (52 - 4\tau^*)B_4(2x-3) + (6\tau^* - 62)B_4(2x-4) +$$

$$(52 - 4\tau^*)B_4(2x-5) + (\tau^* - 26)B_4(2x-6) + 4B_4(2x-7) + B_4(2x-8)),$$

$$\psi_3(x) = 2\tau_3(B_4(2x) + 4B_4(2x-1) + (\rho - 26)B_4(2x-2) + (\tau - 4\rho + 44)B_4(2x-3) + (7\rho - 4\tau - 31)B_4(2x-4) +$$

$$(16 + 6\tau - 8\rho)B_4(2x-5) + (7\rho - 4\tau - 31)B_4(2x-6) + (\tau - 4\rho + 44)B_4(2x-7) +$$

$$(\rho - 26)B_4(2x-8)) + 4B_4(2x-9) + B_4(2x-10)),$$

where $\rho = 21 + \tau/8$.

The conditions of the OEP are satisfied and so the system $X(\{\psi_1, \psi_2, \psi_3\})$ is a tight frame for $L^2(\mathbb{R})$ that has vanishing moments of order $m_0 = 4$. The approximation order of the framelet system is $min\{4, 8\} = 4$.

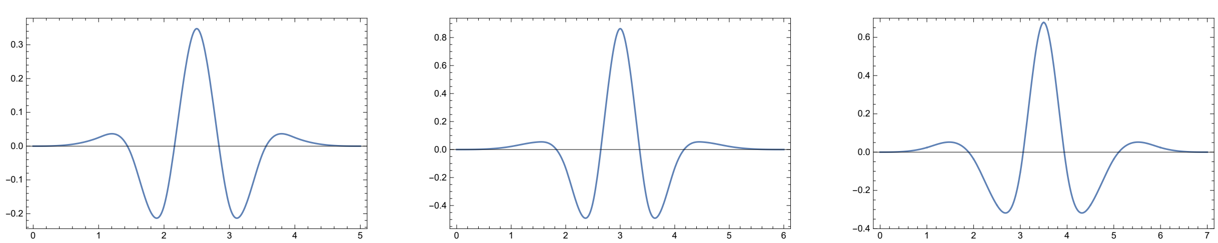

(A) ψ_1 (B) ψ_2 (C) ψ_3

FIGURE 3. The graphs of the symmetric framelets derived from the cubic B-spline, $B_4(x)$ and OEP in Example 3.3.

4. Numerical Procedure

In this section, we present our method which consists of reducing the Voltera-Fredholm Integral Equation to a set of algebraic equations by expanding the unknown function by B-spline framelets with unknown coefficients. The generated system is ill-conditioned so the Moore-Penrose inverse operator method is used to evaluate the unknown coefficients.

Consider the Voltera-Fredholm Integral Equation

$$u(x) = f(x) + \int_0^x K_1(x,t)u(t)dt + \int_0^1 K_2(x,t)u(t)dt, \qquad 0 \le t \le x \le 1, \tag{8}$$

where u is an unknown function and $f \in L^2[0,1]$, $K_1 \in L^2([0,1][0,1])$ and $K_2 \in L^2([0,1][0,1])$ are explicitly known. According to the proposed method, the approximate solution is given by

$$u_n(x) = \sum_{l=1}^{r} \sum_{j<n} \sum_{k\in\mathbb{Z}} c_{l,j,k} \psi_{l,j,k}(x). \tag{9}$$

Substituting Eq.(9) into Eq.(8) yields

$$\sum_{l=1}^{r} \sum_{j<n} \sum_{k\in\mathbb{Z}} c_{l,j,k} \psi_{l,j,k}(x) = f(x) + \sum_{l=1}^{r} \sum_{j<n} \sum_{k\in\mathbb{Z}} c_{l,j,k} \left[\int_a^x K_1(x,t)\psi_{l,j,k}(t)dt + \int_a^b K_2(x,t)\psi_{l,j,k}(t)dt \right].$$

Which can be rearranged to

$$\sum_{l=1}^{r} \sum_{j<n} \sum_{k\in\mathbb{Z}} c_{l,j,k} \left(\psi_{l,j,k}(x) - \left[\int_a^x K_1(x,t)\psi_{l,j,k}(t)dt + \int_a^b K_2(x,t)\psi_{l,j,k}(t)dt \right] \right) = f(x) \tag{10}$$

By producing the collocation points on the interval $[0,1]$

$$x_i = \frac{1}{q} i, \quad i = 0,1,\dots,q, \tag{11}$$

and putting (11) in Eq.(10) we get

$$\sum_{l=1}^{r} \sum_{j<n} \sum_{k\in\mathbb{Z}} c_{l,j,k} \left(\psi_{l,j,k}(x_i) - \left[\int_a^{x_i} K_1(x_i,t)\psi_{l,j,k}(t)dt + \int_a^b K_2(x_i,t)\psi_{l,j,k}(t)dt \right] \right) = f(x_i). \tag{12}$$

Now, we can write Eq.(12) in the form

$$\sum_{l=1}^{r} \sum_{j<n} \sum_{k\in\mathbb{Z}} c_{l,j,k} \mathscr{M}_{l,j,k}(x_i) = f(x_i),$$

where

$$\mathscr{M}_{l,j,k} = \left(\psi_{l,j,k}(x_i) - \left[\int_a^{x_i} K_1(x_i,t)\psi_{l,j,k}(t)dt + \int_a^b K_2(x_i,t)\psi_{l,j,k}(t)dt \right] \right).$$

Rewriting Eq.(12) in matrix form leads to

$$\mathscr{M}c = \mathscr{F},$$

where

$$\mathscr{M} = (\mathscr{M}_{l,j,k}),\ \ c = (c_{l,j,k}),\ \ \mathscr{F} = (f(x_i)).$$

The values of the index k and consequently the number of nodes q depend on the support of the refinable function and the domain of the desired function, i.e. $u(x)$. More specifically, by considering the B_2 framelet system, we have to choose k such that $0 < 2^j x - k < 2$ for $x \in (0,1),\ j = -n+1, -n+2, \ldots, n-1$ and hence suitable values of k are $-2^{n-2}, -2^{n-2}+1, \ldots, 2^{n-1}-1$. In other words, the matrix $\mathscr{M}$ is given by

$$\mathscr{M} = \begin{bmatrix} \mathscr{M}_{1,-n+1,-2^{n-2}}(x_0) & \ldots & \mathscr{M}_{1,-n+1,2^{n-1}-1}(x_0) & \mathscr{M}_{1,-n+2,-2^{n-2}}(x_0) & \ldots & \mathscr{M}_{r,n-1,2^{n-1}-1}(x_0) \\ \mathscr{M}_{1,-n+1,-2^{n-2}}(x_1) & \ldots & \mathscr{M}_{1,-n+1,2^{n-1}-1}(x_1) & \mathscr{M}_{1,-n+2,-2^{n-2}}(x_1) & \ldots & \mathscr{M}_{r,n-1,2^{n-1}-1}(x_1) \\ \vdots & \ddots & \vdots & \ddots & \vdots & \vdots \\ \mathscr{M}_{1,-n+1,-2^{n-2}}(x_q) & \ldots & \mathscr{M}_{1,-n+1,2^{n-1}-1}(x_q) & \mathscr{M}_{1,-n+2,-2^{n-2}}(x_q) & \ldots & \mathscr{M}_{r,n-1,2^{n-1}-1}(x_q) \end{bmatrix},$$

whereas

$$c = \begin{pmatrix} c_{1,-n+1,-2^{n-2}} \\ \vdots \\ c_{1,-n+1,2^{n-1}-1} \\ c_{1,-n+2,-2^{n-2}} \\ \vdots \\ c_{r,n-1,2^{n-1}-1} \end{pmatrix}.$$

As a consequence of sparseness of the matrix $\mathscr{M}$ and the absence of inverse, we computed the unknown coefficients by

$$c = \mathscr{M}^{+}\mathscr{F},$$

where $\mathscr{M}^{+}$ is the Moore-Penrose inverse of $\mathscr{M}$ satisfying

$$\mathscr{M}\mathscr{M}^{+}\mathscr{M} = \mathscr{M}.$$

5. Numerical Experiments

In this section, several numerical examples have been given to illustrate the efficiency of the proposed method. All computations and plotting are accomplished using Mathematica [19].

Example 5.1. Consider the following Volterra-Fredholm Integral Equation [20]

$$u(x) = f(x) + \int_0^x e^{x-t}\, u(t)dt - \int_0^1 e^{x+t}\, u(t)dt, \qquad 0 \le t \le x \le 1,$$

where $f(x) = x^2 + (e-4)\, e^x + x^2 + 2x + 2$. The exact solution of this equation is $u(x) = x^2$. In Table 1, the exact values of the solution at equidistant nodes are compared with its numerical results obtained by the proposed method using B_2 framelets constructed by UEP for $n = 3$ and $n = 4$. It can be seen from the table that as n increases the approximation solution converges toward the exact solution.

x_i	Exact Value	$u_3(x_i)$	$u_4(x_i)$	$\|u_3(x_i) - u(x_i)\|$	$\|u_4(x_i) - u(x_i)\|$
0.0	0.00	-0.002233	-0.000531	2.233e−3	5.305e−4
0.1	0.01	0.009895	0.010269	1.054e−4	2.687e−4
0.2	0.04	0.041118	0.039978	1.118e−3	2.209e−5
0.3	0.09	0.091145	0.089962	1.145e−3	3.800e−5
0.4	0.16	0.159872	0.160286	1.283e−4	2.868e−4
0.5	0.25	0.247376	0.249327	2.624e−3	6.730e−4
0.6	0.36	0.359857	0.360237	1.347e−4	2.372e−4
0.7	0.49	0.491133	0.489977	1.133e−3	2.335e−5
0.8	0.64	0.641100	0.641434	1.100e−3	1.434e−3
0.9	0.81	0.809872	0.809735	1.282e−4	2.653e−4
1.0	1.00	0.997740	0.997716	2.260e−3	2.264e−3

TABLE 1. Comparison between exact solution and approximate solution by the B_2-spline framelets constructed by UEP for Example 5.1

For $n = 4$, Figure 4 shows a good agreement between the exact and approximate solution .

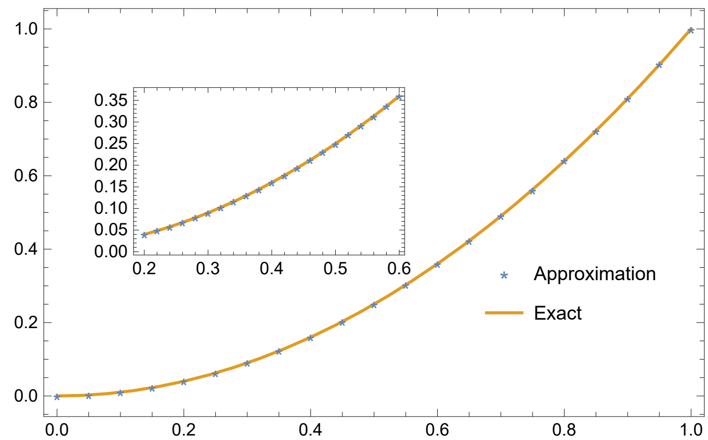

FIGURE 4. Exact and approximate solution for Example 5.1, $n = 4$

.

Example 5.2. Consider the following Volterra-Fredholm Integral Equation [21]

$$u(x) = \frac{2}{3}x - \frac{1}{3}x^4 + \int_0^x x\,t\,u(t)dt + \int_0^1 x\,t\,u(t)dt, \qquad 0 \le t \le x \le 1,$$

with the exact solution $u(x) = x$. For $n = 3$, Table 2 shows the absolute errors at equidistant nodes for the different framelet systems discussed in this paper. The table gives that the increase in the approximation order of the framelet from Examples 3.1 to 3.3 does not improve the absolute error. The table shows that the method described in this paper is a very good technique to solve linear Volterra-Fredholm Integral Equation.

In Table 3 we have compared the absolute errors at equidistant nodes of the proposed method with those from the hybrid orthonormal Bernstein and block puls function (OBH) [22] for $n = 3$. The table shows that the performance of our method is better than that of OBH.

For $n = 3$, Figure 5 shows the absolute errors of the present method via framelets based on B_4-spline and constructed by OEP. This Figure shows that the error is of order 10^{-15}.

Example 5.3. Consider the following Volterra-Fredholm Integral Equation

$$u(x) = \frac{1}{30}(e^x(32 - e^2 - e^{2x})) + \frac{1}{15}\int_0^x e^{x+t}u(t)dt + \frac{1}{15}\int_0^1 e^{x+t}u(t)dt, \qquad 0 \le t \le x \le 1,$$

x_i	B_2, UEP	B_4, UEP	B_4, OEP
0.0	2.62e−16	4.44e−16	3.27e−16
0.1	3.61e−16	2.78e−16	2.50e−16
0.2	3.61e−16	3.33e−16	1.39e−16
0.3	3.89e−16	3.33e−16	3.89e−16
0.4	6.11e−16	5.00e−16	6.66e−16
0.5	6.66e−16	4.44e−16	5.55e−16
0.6	9.99e−16	6.66e−16	6.66e−16
0.7	1.44e−15	1.32e−15	7.77e−16
0.8	1.55e−15	1.33e−15	1.11e−15
0.9	1.78e−15	1.22e−15	1.22e−15
1.0	2.44e−15	1.78e−15	1.55e−15

TABLE 2. Absolute errors for Example 5.2

x_i	OBH	B_4, OEP
0.1	3e−8	2.50e−16
0.2	1e−8	1.39e−16
0.3	1e−8	3.89e−16
0.4	2e−8	6.66e−16
0.5	1e−8	5.55e−16
0.6	1e−8	6.66e−16
0.7	1e−8	7.77e−16
0.8	1e−8	1.11e−15
0.9	7e−8	1.22e−15

TABLE 3. Comparison of the absolute errors with OBH [22] for Example 5.2

with the exact solution $u(x) = e^x$. Here, we use the framelet system based on B_4-spline constructed by OEP to determine the approximate solutions. In Table 4 we have compared the

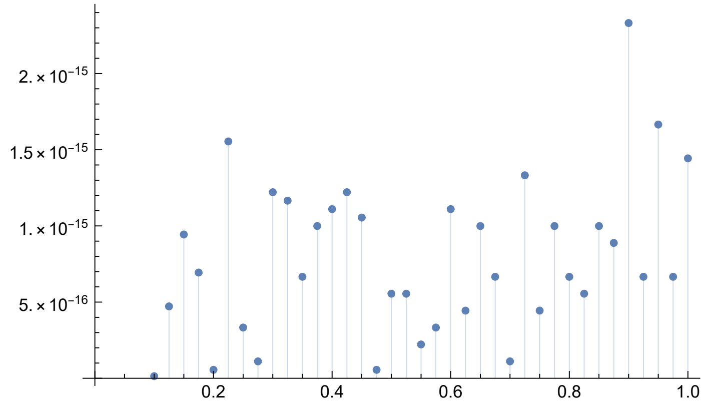

FIGURE 5. Absolute errors of the approximate solution in Example 5.2 for $n = 3$

absolute errors of the proposed method with those from the Taylor expansion method [23]. The table shows that the performance of our method is better than that of the Taylor expansion method.

x_i	Taylor Expansion	B_4, OEP
0.1	1.75e−3	1.65e−7
0.2	1.49e−3	3.15e−7
0.3	1.22e−3	3.23e−7
0.4	9.60e−4	5.69e−8
0.5	7.10e−4	5.90e−7
0.6	4.82e−4	1.34e−7
0.7	2.86e−4	3.89e−7
0.8	1.33e−4	6.72e−7
0.9	3.49e−5	2.88e−7
1.0	1.12e−6	1.71e−7

TABLE 4. Comparison of the absolute errors with the Taylor expansion method [23] for Example 5.3

6. Conclusion

In this paper, the linear Volterra-Fredholm Integral Equation is solved by using B-spline based framelets and collocation method. In the proposed technique, the unknown function $u(x)$ is approximated using framelets and the integral equation is converted to a system of algebraic equations. The efficiency of the presented method has been tested through several numerical examples.

Conflict of Interests

The author(s) declare that there is no conflict of interests.

References

[1] Y.G. Wang, X. Zhuang, Tight framelets on graphs for multiscale data analysis, in: Y.M. Lu, M. Papadakis, D. Van De Ville (Eds.), Wavelets and Sparsity XVIII, SPIE, San Diego, United States, 2019: p. 11.

[2] Z. Shen, Wavelet Frames and Image Restorations, in: Proceedings of the International Congress of Mathematicians 2010 (ICM 2010), Published by Hindustan Book Agency (HBA), India. WSPC Distribute for All Markets Except in India, Hyderabad, India, 2011: pp. 2834–2863.

[3] I. Daubechie, B. Han, Pairs of Dual Wavelet Frames from Any Two Refinable Functions, Construct. Approx. 20 (2004), 325–352.

[4] B. Han, Q. Mo, Tight wavelet frames generated by three symmetric B-spline functions with high vanishing moments, Proc. Amer. Math. Soc. 132 (2003), 77–86.

[5] I.W. Selesnick, A.F. Abdelnour, Symmetric wavelet tight frames with two generators, Appl. Comput. Harmonic Anal. 17 (2004), 211–225.

[6] R.J. Duffin, A.C. Schaeffer, A class of nonharmonic Fourier series, Trans. Amer. Math. Soc. 72 (1952), 341–341.

[7] I. Daubechies, A. Grossmann, Y. Meyer, Painless nonorthogonal expansions, J. Math. Phys. 27 (1986), 1271–1283.

[8] A. Ron, Z. Shen, Affine systems in $L_2(R^d)$: the analysis of the analysis operator, J. Funct. Anal. 148 (2) (1997), 408–447.

[9] B. Adcock, D. Huybrechs, Frames and numerical approximation, SIAM Rev. 61 (3) (2019) 443–473.

[10] I. Daubechies, B. Han, A. Ron, Z. Shen, Framelets: MRA-based constructions of wavelet frames, Appl. Comput. Harmonic Anal. 14 (2003), 1–46.

[11] B. Dong, Z. Shen, MRA based wavelet frames and applications. IAS Lecture Notes Series, Summer Program on "The Mathematics of Image Processing". Park City Mathematics Institute, Salt Lake City (2010).

[12] M.A. Abdou, A.A. Soliman, M.A. Abdel–Aty, On a discussion of Volterra–Fredholm integral equation with discontinuous kernel, J. Egypt Math. Soc. 28 (2020), 11.

[13] Y. Al-Jarrah, On the approximation solutions of linear and nonlinear volterra integral equation of first and second kinds by using b-spline tight framelets generated by unitary extension principle and oblique extension principle, Int. J. Differ. Equ. 15 (2) (2020), 165–189.

[14] R. Amin, K. Shah, M. Asif, I. Khan, Efficient numerical technique for solution of delay volterra-fredholm integral equations using haar wavelet, Heliyon 6 (10) (2020), e05108.

[15] E. Banifatemi, M. Razzaghi, S. Yousefi, Two-dimensional legendre wavelets method for the mixed volterra-fredholm integral equations, J. Vibrat. Control, 13 (11) (2007), 1667–1675.

[16] A.-M. Wazwaz, A reliable treatment for mixed volterra–fredholm integral equations, Appl. Math. Comput. 127 (2-3) (2002), 405–414.

[17] M. Mohammad, C. Cattani, A collocation method via the quasi-affine biorthogonal systems for solving weakly singular type of volterra-fredholm integral equations, Alex. Eng. J. 59 (4) (2020), 2181–2191.

[18] O. Christensen, An introduction to frames and Riesz bases, Vol. 7, Springer, New York, 2003.

[19] Wolfram, Mathematica, Version 12.2, `https://www.wolfram.com/mathematica`.

[20] X. Tang, Numerical solution of volterra–fredholm integral equations using parameterized pseudospectral integration matrices, Appl. Math. Comput. 270 (2015), 744–755.

[21] Y. Al-Jarrah, E.-B. Lin, Numerical solution of fredholm-volterra integral equations by using scaling function interpolation method, Appl. Math. 4 (1) (2013), 204–209.

[22] M.A. Ramadan, M.R. Ali, Numerical solution of volterra-fredholm integral equations using hybrid orthonormal bernstein and block-pulse functions, Asian Res. J. Math. (2017), 1–14.

[23] M. Didgar, A. Vahidi, Approximate solution of linear volterra-fredholm integral equations and systems of volterra-fredholm integral equations using taylor expansion method, Iran. J. Math. Sci. Inform. 15 (2) (2020), 31–50.